

Experimental and Theoretical Studies of $\text{Ni}_n(\text{C}_2\text{H}_4)_m$. Synthesis, Vibrational and Electronic Spectra, and Generalized Valence Bond–Configuration Interaction Studies. The Metal Atom Chemistry and a Localized Bonding Model for Ethylene Chemisorbed on Bulk Nickel

G. A. Ozin,*¹ W. J. Power, T. H. Upton, and W. A. Goddard III*

Contribution from Lash Miller Chemistry Laboratories and Erindale College, University of Toronto, Toronto, Ontario, Canada, and Arthur Amos Noyes Laboratory of Chemical Physics,² California Institute of Technology, Pasadena, California 91125. Received July 23, 1977

Abstract: Using cryochemical manipulation of Ni atom reactions with ethylene–argon mixtures at 15–25 K and from examination of the vibrational and electronic spectra, we have identified $\text{Ni}_2(\text{C}_2\text{H}_4)_m$ (where $m = 1, 2$) in the presence of $\text{Ni}(\text{C}_2\text{H}_4)_m$ (where $m = 1, 2, 3$). These results suggest strongly that the ethylene moiety is complexed to the chemical site in a π -complexed manner, probably in association with only one of the Ni atoms. Some evidence for the formation of $\text{Ni}_x(\text{C}_2\text{H}_4)_y$ with $x \geq 3$ is presented. To further characterize the $\text{Ni}_2(\text{C}_2\text{H}_4)$ complex, we carried out generalized valence bond (GVB) and configuration interaction (CI) calculations on $\text{Ni}(\text{C}_2\text{H}_4)$ and $\text{Ni}_2(\text{C}_2\text{H}_4)$ in the π -coordinate geometry. For both complexes the ethylene geometry is found to be only weakly perturbed, with $R(\text{CC}) = 1.32 \text{ \AA}$ and $R(\text{NiC}) = 2.07 \text{ \AA}$. The CH bonds are found to bend only 2° out of the ethylene molecular plane. There is an increase in ethylene–Ni binding energy upon coordination of the second Ni atom, from 14.2 kcal for $\text{Ni}(\text{C}_2\text{H}_4)$ to 27.2 kcal for $\text{Ni}_2(\text{C}_2\text{H}_4)$. The experimental and theoretical results are discussed with reference to the problem of chemisorption of ethylene on bulk nickel.

I. Introduction

In theoretical and experimental studies of chemisorption and catalysis, a great deal of discussion has focused on the validity of employing localized models for elucidating the surface bonding between adsorbate and adsorbent.³ For this model, the chemisorptive bond is described as localized, involving only a limited number of neighboring surface atoms near the adsorbate. This idea receives some support from analogies with a number of organometallic complexes and the homogeneous reactions of these complexes.⁴ However, until very recently, a serious shortcoming of the localized model has been the difficulty of experimentally generating realistic molecular systems for interconnecting the infinite surface molecular state and its finite-cluster localized-bonding counterpart.^{4c,8} Homogeneous catalysts often possess ligands that have no counterpart in bulk systems, and the influence of these ligands on metal atom states and catalytic properties is difficult to measure. While the correspondence between the catalytic properties of organometallic complexes involving small metal clusters and their bulk analogues has been well documented,⁹ attempts to draw more detailed mechanistic and structural comparisons must be made with caution.

In this study we have addressed ourselves to the challenge of producing a more “ideal” localized bonding model for a particular surface interaction, namely, that of ethylene chemisorbed onto bulk nickel. As a model “surface complex” we have chosen to characterize, both experimentally and theoretically, a nickel diatom interacting with an ethylene molecule, namely, $\text{Ni}_2(\text{C}_2\text{H}_4)$. Such a system is a reasonable synthetic goal in view of the recent cryochemical syntheses of Ni_2 ^{8e,11} and $\text{Ni}(\text{C}_2\text{H}_4)_{1,2,3}$ ^{8e} and a comparison of the spectroscopic properties of each system should provide valuable information on the mode of bonding. Similarly, it is possible to draw on recent theoretical studies of Ni_2 ¹² and $\text{Ni}(\text{C}_2\text{H}_4)$ ¹³ as a means to further understand the bonding and structural properties which emerge from the study of $\text{Ni}_2(\text{C}_2\text{H}_4)$.

To date, attempts to determine the mode of bonding for ethylene on bulk nickel have produced conflicting results. The

UV photoemission spectra of adsorbed ethylene^{3d} have been compared with gas-phase spectra, suggesting that the only significant effect of chemisorption is to shift the energy of the π level. From this and related theoretical investigations,¹⁴ Demuth and Eastman concluded that the ethylene–nickel chemisorptive bond involves predominantly π -d interactions without significant distortion of ethylene relative to its gas-phase geometry. The assumption here is that ethylene forms a π complex coordinating symmetrically to a single surface atom as originally proposed for organometallic complexes.¹⁵

However, from earlier infrared investigations and various surface reactions^{10a,b,16,17} it had been inferred that ethylene chemisorbed onto silica-supported nickel exists as a di- σ -surface complex, in which each of the two carbon atoms forms a σ bond to a different nickel atom. This picture has changed slightly as a result of some very recent infrared investigations^{10c,d} that provide evidence for a π -bonded form of ethylene which may coexist with the di- σ form for group 8 supported metals.^{10f} Along with these experimental probes of the chemisorbed state of ethylene have emerged SCF- $X\alpha$ -SW calculations of the electronic structures of model surface ethylene complexes, one involving $\text{M}(\text{C}_2\text{H}_4)$ (where $\text{M} = \text{Ni}, \text{Pd},$ and Pt)^{6b} and the other concerning Ni_2 and $\text{Ni}_2(\text{C}_2\text{H}_4)$,⁷ the latter having ethylene in both a di- σ and π -complexed form.

It is our intention with this study to provide further experimental and theoretical information that should help to resolve this conflict. In what follows, we will first describe in detail (section II) the cryochemical synthesis and spectroscopic characterization of $\text{Ni}_2(\text{C}_2\text{H}_4)$ based on previous experience with Ni_2 ,¹⁸ Ni_2 ,^{8e,11} and $\text{Ni}(\text{C}_2\text{H}_4)_{1,2,3}$.^{8e} In section III we present the results of generalized valence bond (GVB) and configuration interaction (CI) calculations for the $\text{Ni}_2(\text{C}_2\text{H}_4)$ complex with reference to similar studies on Ni_2 ¹² and $\text{Ni}(\text{C}_2\text{H}_4)$.¹³ In section IV we will discuss our results in light of other theoretical studies and will consider the importance of isomeric structures for the $\text{Ni}_2(\text{C}_2\text{H}_4)$ complex. Finally, in section V, the implications of the results for this “ligand-free” finite complex on the bulk chemisorption problem will be considered.

Table I. Relevant γ_{CC} and δ_{CH_2} Vibrational Modes of $Ni(C_2H_4)_n$ and $Ni_2(C_2H_4)_m$ Species ($n = 1, 2, 3$; $m = 1, 2$)

$Ni(C_2H_4)_n^a$	$Ni(C_2H_4)_2^a$	$Ni(C_2H_4)_3^a$	$Ni_2(C_2H_4)_m^{b,d}$	$Ni_2(C_2H_4)_2^{b,d}$	mode ^c
1499	1465	1514	1488	1504	$\nu_{C=C}$
1160	1223	1246	1208	1232	δ_{CH_2}
			1180		

^a A complete list of vibrational frequencies and assignments for these species is given in ref 6e. ^b A species absorbing at 1508/1240 cm^{-1} could be a matrix split component of $Ni_2(C_2H_4)_2$. A structural isomer is also possible as is a higher stoichiometry species such as $Ni_2(C_2H_4)_3$ (see text). ^c Frequencies in cm^{-1} . ^d ν_{CH_2} stretching modes at 2880 and 2908 cm^{-1} can be associated with these species, although their low intensities preclude a specific assignment. The persistence of the ν_{CH_2} band at 910 cm^{-1} after warmup to 30–35 K implies that part of the intensity of this band is attributable to $Ni_2(C_2H_4)_{1or2}$. Low-frequency bands were also observed at 446, 416, 376 cm^{-1} (probably NiC modes) which, from their warmup behavior, appear to belong to *three* different species; the 376 cm^{-1} band seems to parallel the growth–decay properties of $Ni(C_2H_4)_{2,3}$ while those at 446/416 cm^{-1} follow the pattern of $Ni_2(C_2H_4)_2/Ni_2(C_2H_4)$, respectively.

II. Synthesis and Spectroscopic Characterization

A. Experimental. Monatomic Ni vapor was generated by directly heating a 0.020-in. ribbon filament of the metal with ac in a furnace similar to that described previously.¹⁹ The nickel (99.9%) was supplied by McKay, New York, N.Y. Research grade C_2H_4 (99.9%) and Ar (99.9%) were supplied by Matheson of Canada. The rate of Ni atom deposition was continuously monitored using a quartz crystal microbalance.²⁰

In the infrared experiments, matrices were deposited onto a CsI optical plate cooled to 15 K (optimum reaction temperature) by means of an Air Products Displex, closed-cycle helium refrigerator. Infrared spectra were recorded on a Perkin-Elmer 180 spectrophotometer. Ultraviolet–visible spectra were recorded on a standard Varian Techtron in the range 190–900 nm, the sample being deposited onto a NaCl optical window.

B. Results and Discussion. Before describing the intricacies of the $Ni_2(C_2H_4)_m$ problem, we shall present a brief resumé of the background literature with which one should be familiar in order to appreciate our experimental and analytical approach to the cryochemical synthesis of a binuclear nickel-olefin fragment, starting with atomic nickel. To begin, the existence of binary nickel olefin complexes of the form $Ni(ol)_n$ was first demonstrated by Wilke et al.²¹ from the reaction of $Ni(1,5-COD)_2$ and C_2H_4 at $-196^\circ C$. Tris(ethylene)nickel(0), $Ni(C_2H_4)_3$, could be crystallized from liquid ethylene and was found to decompose to metallic nickel and ethylene at $0^\circ C$.²¹ Subsequently, the same compound was directly synthesized²² by cocondensing atomic Ni with C_2H_4 in the temperature range 77–10 K and its infrared, Raman,²³ and UV–visible spectra were recorded. By matrix dilution and warm-up techniques, isotopic ^{13}C and 2H labeling, and metal concentration experiments, the reactive intermediates $Ni(C_2H_4)$ and $Ni(C_2H_4)_2$ were identified and their infrared and UV–visible spectral properties recorded.^{8e} All of these matrix experiments were conducted under extremely high dilution conditions with respect to the nickel, such that mononuclear complex formation predominated.²⁴ The relevant spectroscopic details for $Ni(C_2H_4)_n$ (where $n = 1, 2, 3$) are tabulated for reference purposes in Table I.

1. Nickel Atom–Nickel Diatom Ultraviolet–Visible Experiments. That one is really manipulating atomic nickel in these cryochemical $Ni/C_2H_4/Ar$ reactions can easily be demonstrated by recording the UV–visible spectrum of the corresponding Ni/Ar mixture under identical concentration and deposition conditions.¹⁸ For example, using Ni/Ar $\approx 1/10^4$ dilutions which minimize surface diffusion and metal aggregation processes, one observes at 10 K the optical spectrum shown in Figure 1A. Apart from the usual matrix-induced frequency shifts and band splittings, the majority of the observed absorptions can be reasonably well correlated with the atomic resonance lines of gaseous nickel (see Gruen for details of atomic matrix correlation (AMCOR) techniques).²⁵ In

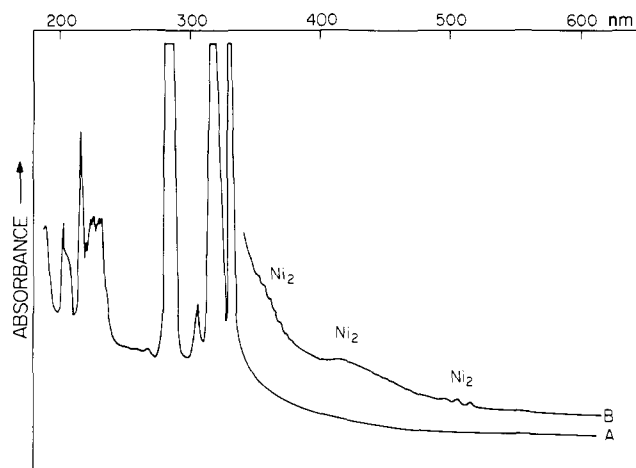


Figure 1. The UV–visible spectrum of Ni/Ar (A) $1/10^4$ and (B) $1/10^3$ matrices at 10 K showing the presence of isolated Ni atoms under high-dilution conditions (A) and both Ni atoms and Ni_2 molecules under lower dilution conditions.

particular, note that the region to energies lower than 330 nm is completely devoid of spectral lines.

On increasing the Ni/Ar matrix ratio by a factor of 10 ($1/10^3$) and recording the optical spectrum at 10 K (Figure 1B) one observes *three* new absorptions in the regions of 350, 420, and 510 nm, besides those previously ascribed to atomic Ni. The 350- and 510-nm bands display associated vibrational fine structure with spacings of the order of 330 and 360 cm^{-1} , respectively. This group of three new absorptions always appears with approximately the same relative intensities under a variety of deposition and warmup conditions. Of particular importance is the fact that they are the first observable spectral lines to develop on entering the nickel concentration regime, which favors appreciable surface diffusion and aggregation effects.²⁶ On the basis of a series of Ni/Ar concentration experiments in the range $1/10^4$ to $1/10^2$ and by comparison with the more complete analysis of Moskovits and Hulse,¹¹ we feel confident in ascribing the three absorptions at 350, 420, and 510 nm to diatomic nickel, Ni_2 . The nature of these transitions may be understood by considering the essential features of the Ni_2 bond.¹² The ground state of the dimer involves $3D(4s^1 3d^9)$ atoms coupled to produce primarily a 4s–4s bond (see section III). Thus diatomic transitions should be of four general types: $3d \rightarrow 4p$, $3d \rightarrow 4s\sigma_u$, $4s\sigma_g \rightarrow 4p$, and $4s\sigma_g \rightarrow 4s\sigma_u$. The observed Ni_2 bands at 350 and 510 nm each exhibit vibrational structure very similar to the ground state,^{12,27} and thus must correspond to transitions that do not strongly perturb the 4s–4s bond. Only $3d \rightarrow 4p$ transitions satisfy this requirement; for atomic Ni these transitions are observed in the regions of 270–320 and 350–390 nm (differing only in the coupling of the open-shell orbitals).²⁸ As such, each set of atomic transitions may be considered as

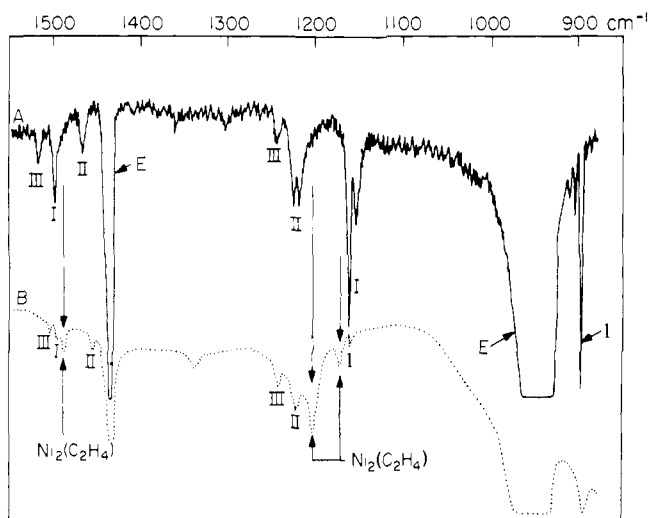


Figure 2. The matrix infrared spectrum observed on depositing Ni atoms with $C_2H_4/Ar \approx 1/50$ mixtures at 15 K with (A) $Ni/Ar \approx 1/10^4$ and (B) $Ni/Ar \approx 1/10^3$ [absorptions associated with free ethylene in the matrix are labeled E and $Ni(C_2H_4)_n$ where $n = 1, 2, 3$ and labeled I, II, III, respectively], showing the formation of $Ni_2(C_2H_4)$.

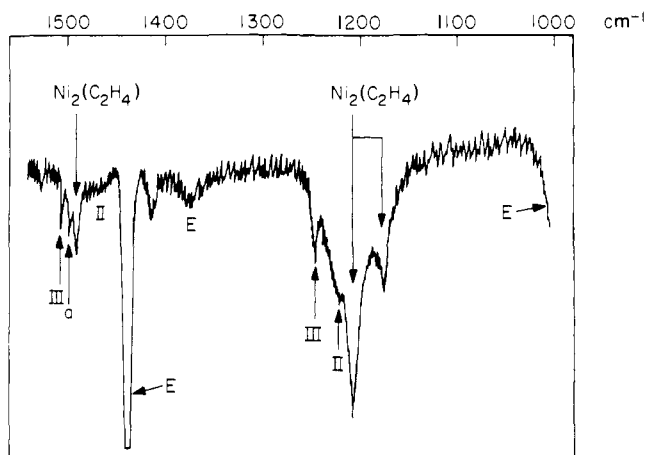


Figure 3. The same as Figure 2B except after matrix annealing to 40–45 K and recooling to 10 K [“a” represents either a trace of I or the new species $Ni_2(C_2H_4)_2$ (see text)].

the source of the observed features at 350 and 510 nm, respectively. The structureless band at 420 nm is more ambiguous. Disruption of the 4s–4s bond is suggested by the band shape; however, transitions from any of the four types listed could produce this effect, and none can presently be eliminated from consideration (preliminary matrix photochemical experiments of samples containing Ni and Ni_2 suggest that 420-nm radiation leads to dissociation of Ni_2 and regeneration of atomic nickel).⁵⁰

2. Infrared Experiments. Having established the experimental conditions required to generate appreciable amounts of Ni_2 in Ar, we proceeded to perform a series of $Ni/C_2H_4/Ar$ concentration experiments in an effort to identify binuclear $Ni_2(C_2H_4)_n$ species in the presence of the previously identified complexes of $Ni(C_2H_4)_n$. By operating in the $C_2H_4/Ar \approx 1/50$ concentration range [which under $Ni/Ar \approx 1/10^4$ conditions favors mononuclear $Ni(C_2H_4)_{1,2}$] we hoped that by examining $Ni/Ar \approx 1/10^3$ to $1/10^2$ depositions we would be able to identify low-stoichiometry binuclears, such as $Ni_2(C_2H_4)_{1,2}$. In these experiments, the most intense and definitive vibrational modes for identifying new products turned

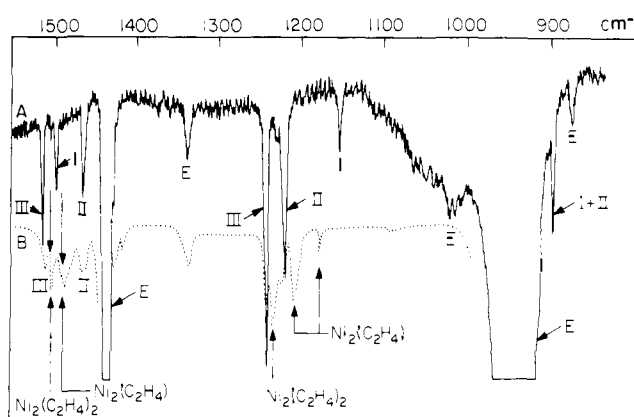


Figure 4. The matrix infrared spectrum observed on depositing Ni atoms with (A) $C_2H_4/Ar \approx 1/10$ mixtures at 15 K with $Ni/Ar \approx 1/10^4$ and (B) $C_2H_4/Ar \approx 1/25$ mixtures at 15 K with $Ni/Ar \approx 1/10^3$ showing the formation of $Ni_2(C_2H_4)$ and $Ni_2(C_2H_4)_2$.

out to be ν_{CC} stretching and δ_{CH_2} deformations. The results of a typical infrared experiment under mononuclear conditions are displayed in Figure 2A, whereas those under combined mononuclear/binuclear conditions are shown in Figure 2B. Besides the ν_{CC} and δ_{CH_2} of $Ni(C_2H_4)$ (1499 and 1160 cm^{-1}) and $Ni(C_2H_4)_2$ (1465 and 1223 cm^{-1}), labeled I and II, respectively, in Figure 2B, one notices the conspicuous appearance of a new ν_{CC} stretching mode at 1488 cm^{-1} and new δ_{CH_2} deformational modes at 1208/1180 cm^{-1} . These absorptions always appear with approximately the same intensities under a variety of deposition conditions (vide infra) and display parallel growth and decay behavior during matrix annealing. It is particularly noteworthy that this new species appears to dominate the spectrum on warming $C_2H_4/Ar \approx 1/50$ mixtures to 35 K. Further warming to 40–45 K causes the ν_{CC} stretching mode of $Ni(C_2H_4)_2$ at 1465 cm^{-1} as well as the δ_{CH_2} of $Ni(C_2H_4)$ at 1160 cm^{-1} to essentially decay to zero with the concomitant growth of the ν_{CC} of $Ni(C_2H_4)_3$ at 1514 cm^{-1} (Figure 3). The persistence of the bands around 1232 and 1504 cm^{-1} [which cannot be associated with $Ni(C_2H_4)_2$ and $Ni(C_2H_4)$, respectively, at this stage of the experiment]^{8e} suggests but does not prove the presence of a second new species (vide infra). Since the new species absorbing at 1488, 1208, and 1180 cm^{-1} only appears under reaction conditions favoring binuclear complex formation and since there is a carbon–carbon stretching mode in the 1500- cm^{-1} region, we assign this species as $Ni_2(C_2H_4)$ containing a π -complexed form of ethylene.

Further evidence for the assignment of the lowest ethylene stoichiometry binuclear stems from experiments in $C_2H_4/Ar \approx 1/10$ to $1/50$ with $Ni/Ar \approx 1/10^4$ to $1/10^2$. A typical infrared trace at $C_2H_4/Ar \approx 1/10$ is shown in Figure 4A under Ni/Ar conditions which favor mononuclear complex formation, from which the characteristic absorptions of $Ni(C_2H_4)$ (1496 and 1158 cm^{-1}), $Ni(C_2H_4)_2$ (1465, 1235, and 1224 cm^{-1}), and $Ni(C_2H_4)_3$ (1514 and 1246 cm^{-1}) are easily recognized. By moving to Ni/Ar conditions which favor mononuclear and binuclear complex formation and using $C_2H_4/Ar \approx 1/25$, we obtain infrared spectra of the type shown in Figure 4B. Note especially under these conditions the spectroscopic absence of $Ni(C_2H_4)$, which is best appreciated by the inability to detect the characteristic δ_{CH_2} mode at 1160 cm^{-1} . Of particular significance in Figure 4B is the appearance of two new ν_{CC} modes at 1488 and 1504 cm^{-1} which appear to go together with the new δ_{CH_2} modes at 1232 and 1208, 1180 cm^{-1} , respectively. This can be illustrated from a typical warmup experiment to 30 and 35 K which shows the growth of the 1504,

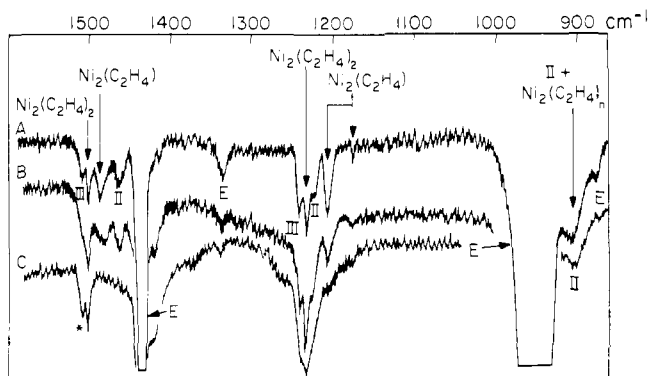


Figure 5. (A) The same as Figure 4B, (B–C) the effect of 30 and 35 K annealing. The asterisk probably indicates a matrix site splitting of $Ni_2(C_2H_4)_2$ rather than evidence for a higher stoichiometry binuclear $Ni_2(C_2H_4)_m$ where $m > 2$.

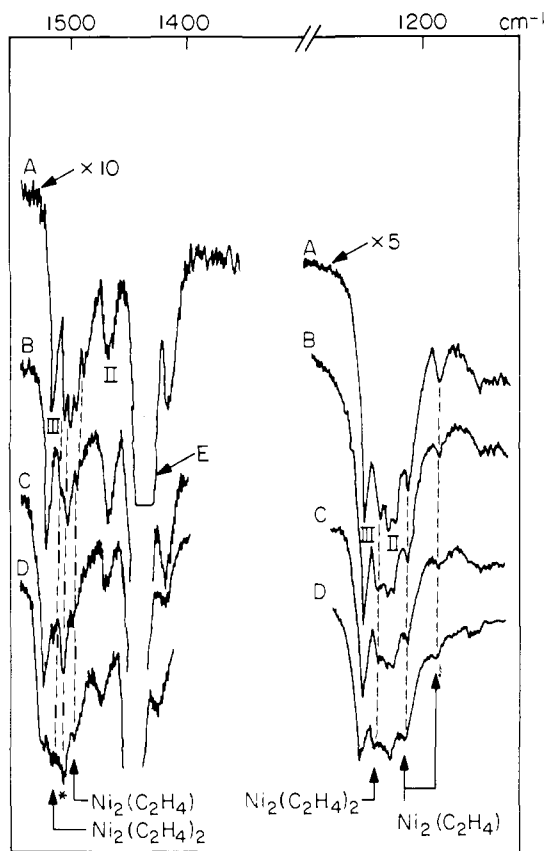


Figure 6. (A) The same as Figure 2B except that $C_2H_4/Ar \approx 1/10$ mixtures were used. (B–D) represent a series of warmup experiments to 25, 30, and 35 K, respectively, and recoiling to 10 K for spectral recording.

1232 cm^{-1} pair at essentially the same rate, concomitant with the decay of the $1488, 1208, 1180\text{ cm}^{-1}$ group of absorptions associated with the low-stoichiometry fragment $Ni_2(C_2H_4)$ (Figure 5B). Therefore the results of high Ni concentration $C_2H_4/Ar \approx 1/50$ to $1/25$ experiments provide convincing evidence that *two* binuclear binary nickel ethylene complexes can be generated, most probably containing *one* and *two* π -complexed ethylene ligands, that is, $Ni_2(C_2H_4)$ and $Ni_2(C_2H_4)_2$, respectively. A small splitting observed on the ν_{CC} mode of $Ni_2(C_2H_4)_2$ at 1508 and 1504 cm^{-1} probably represents a matrix site effect rather than evidence for a higher stoichiometry mononuclear (vide infra).

Similar experiments performed in $C_2H_4/Ar \approx 1/10$ matrices and $Ni/Ar \approx 1/10^4$ to $1/10^2$ generally confirmed the above proposals. On deposition at 15 K, apart from the char-

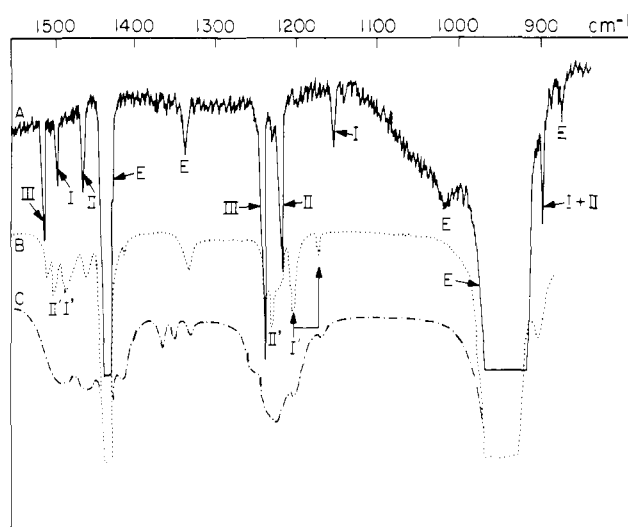


Figure 7. The matrix infrared spectrum observed on depositing Ni atoms (A) with $C_2H_4/Ar \approx 1/10$ mixtures at 15 K with $Ni/Ar \approx 1/10^4$, (B) with $C_2H_4/Ar \approx 1/25$ mixtures at 15 K with $Ni/Ar \approx 1/10^3$, and (C) $Ni/Ar \approx 1/10^2$ showing the formation of $Ni_2(C_2H_4)$ (denoted as I) and $Ni_2(C_2H_4)_2$ (denoted as II) and the gradual progression from $Ni(C_2H_4)_n$ to $Ni_2(C_2H_4)_n$ to $Ni_x(C_2H_4)_n$ (where $x \approx 3$).

acteristic ν_{CC} and δ_{CH_2} modes of $Ni(C_2H_4)_2$ and $Ni(C_2H_4)_3$,^{8e} one observes *only* those ascribed earlier to $Ni_2(C_2H_4)$ and $Ni_2(C_2H_4)_2$ (Figure 6A). As seen in the $1/25$ experiments, a small splitting is again observed on the ν_{CC} mode of $Ni_2(C_2H_4)_2$ at $1508, 1504\text{ cm}^{-1}$ and is probably best ascribed to a matrix site effect rather than evidence for a higher stoichiometry binuclear (Figure 6).

Finally, it is worth commenting briefly on the effect of increasing the Ni/Ar ratio into the range $1/10^2$ to $1/10$ and the deposition temperature from 15 to 25 K. From a UV-visible point of view the Ni/Ar spectrum “in the absence of C_2H_4 ” shows the growth of a *new* absorption centered at roughly 460 nm with vibrational fine structure and an average spacing of approximately 200 cm^{-1} . In accordance with the work of Moskovits and Hulse¹¹ we feel confident that this new absorption is probably best associated with the second stage of the nickel aggregation process, namely, to trinickel, Ni_3 . We refer the reader to ref 11 for details of the Ni_3 analysis and note in passing that an earlier Ni/Ar report by De Vore et al.²⁹ of a band at 460 nm with an average vibrational spacing of 192 cm^{-1} and an assignment to Ni_2 is probably incorrect. On the basis of our experiments and those of Moskovits and Hulse,¹¹ the 460-nm absorption is best assigned to Ni_3 .

By experimenting with $Ni/C_2H_4/Ar$ cocondensations under conditions which favor the presence of some Ni_3 , we observe a general broadening of the infrared ν_{CC} and δ_{CH_2} modes in the region of $1520\text{--}1450$ and $1250\text{--}1180\text{ cm}^{-1}$, respectively (Figure 7). The breadth of the spectral absorbances and the generally ill-defined nature of the infrared spectra preclude a definitive assignment to a particular $Ni_3(C_2H_4)_p$ species. However, it is pertinent to note that on passing from $Ni(C_2H_4)_n$ to $Ni_2(C_2H_4)_m$ experimental conditions, a noticeable increase in the ν_{CC} and δ_{CH_2} bandwidths is experienced (Figure 7B) which becomes even more pronounced under conditions which favor $Ni_3(C_2H_4)_p$ and higher cluster species (Figure 7C). In fact the general crowding of infrared-active ν_{CC} and δ_{CH_2} modes around the $1500, 1220\text{ cm}^{-1}$ spectral regions closely extrapolates to the situation experienced for C_2H_4 chemisorbed on group 8 supported metals.¹⁰

These observations, in conjunction with the presence of ν_{CC} stretching modes in the 1500-cm^{-1} region for $Ni_x(C_2H_4)_y$ (where $x = 1, 2, 3$) taken in combination with the general

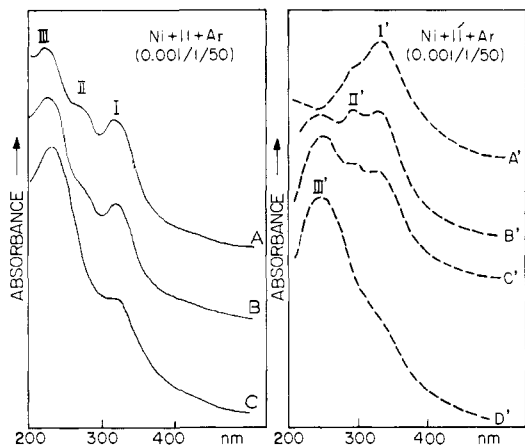


Figure 8. The UV-visible spectra obtained on depositing Ni atoms with (A) $C_2H_4/Ar \approx 1/50$ and (A') $C_3H_6/Ar \approx 1/50$ mixtures with $Ni/Ar \approx 1/10^4$ at 15 K; (B-C) and (B'-D') the effects of warming these matrices in the range 20–35 K, showing the initial formation of $Ni(C_2H_4)$ (I) and $Ni(C_3H_6)$ (I') and the gradual conversion to $Ni(C_2H_4)_2$ (II), $Ni(C_3H_6)_2$ (II'), and $Ni(C_2H_4)_3$ (III), $Ni(C_3H_6)_3$ (III') where C_3H_6 is propylene.²³

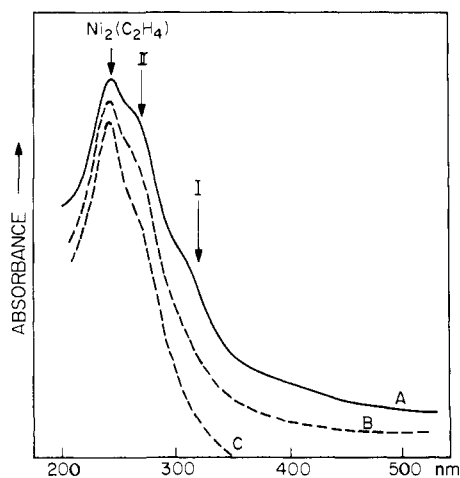


Figure 9. The matrix UV-visible spectrum observed (A) on depositing Ni atoms with a $C_2H_4/Ar \approx 1/50$ mixture at 15 K with $Ni/Ar \approx 1/10^3$ and (B-C) after warming the matrix to 30 and 40 K, respectively, and recoiling to 10 K for spectral recording purposes [I and II represent traces of $Ni(C_2H_4)$ and $Ni(C_2H_4)_2$, respectively].

similarity of the vibrational spectra of these small nickel-ethylene cluster complexes, provide convincing support for a localized bonding description of ethylene chemisorbed on nickel and a π -nickel-ethylene interaction (vide infra).

3. Ultraviolet-Visible Experiments. Recall that on depositing Ni atoms with $C_2H_4/Ar \approx 1/50$ mixtures at 15 K, under metal concentration conditions favoring mononuclear complex formation ($Ni/Ar \approx 1/10^4$), one observes an optical spectrum dominated by an intense UV absorption centered at roughly 320 nm.⁸⁸ The corresponding infrared data imply that this UV band is associated with $Ni(C_2H_4)$.^{8e} A typical series of optical spectra for the mononuclear complexes $Ni(C_2H_4)_n$ [and for comparison $Ni(C_3H_6)_n$] obtained under these dilute conditions is shown in Figure 8. The spectra were recorded under constant concentration conditions for a variety of temperatures in the range 15–40 K and serve to illustrate the predominance of the monoolefin species upon deposition and the subsequent conversion to the bis and tris olefin complexes on matrix annealing. Increasing the Ni concentration to the range $Ni/Ar \approx 1/10^3$ while holding $C_2H_4/Ar \approx 1/50$ enhances the formation of $Ni_2(C_2H_4)$, and we observe optical spectra of the type shown in Figure 9A, in which the 320-nm absorption of $Ni(C_2H_4)$ no

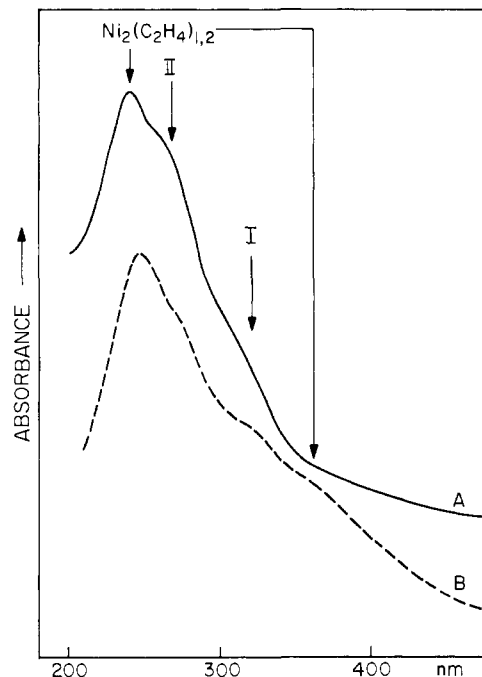


Figure 10. The same as Figure 9A and B showing the effect of increasing the Ni concentration (twofold) and deposition temperature (25 K).

longer dominates the spectrum. Instead, an intense UV absorption peaking at roughly 243 nm with a noticeable shoulder at about 314 nm are the most prominent spectral features, with the 280-nm band of $Ni(C_2H_4)_2$ appearing as a shoulder. On warming these matrices to 30–40 K, the 280-nm shoulder and the 320-nm band tend to decay (Figure 9B) which parallels the warmup behavior observed for $Ni(C_2H_4)$ in the presence of $Ni_2(C_2H_4)$ (see section II.B.2). On these grounds we feel reasonably confident in assigning the 243-nm absorption to $Ni_2(C_2H_4)$. Experiments performed at higher C_2H_4/Ar ratios and higher temperature depositions 20–25 K [designed to enhance the generation of $Ni_2(C_2H_4)_2$] produce a noticeable broad spectral feature in the region of 370 nm (Figure 10) which cannot be attributed to either $Ni(C_2H_4)_{1,2,3}$ ^{8e,g} or $Ni_2(C_2H_4)$. We tentatively assign this band to an electronic transition associated with the presence of the Ni-Ni bond in $Ni_2(C_2H_4)_2$, although one cannot be confident that band overlap in the 200–300-nm region has not obscured any other spectral characteristics of $Ni_2(C_2H_4)_2$.³⁰ The nature of these intense UV bands is difficult to determine, and we will defer discussion of them until the bonding in these finite clusters has been described.

III. The Generalized Valence Bond Description of $Ni_2(C_2H_4)$

Before discussing the bonding and spectral properties of the $Ni_2(C_2H_4)$ complex itself, we will first consider these same properties for the various molecular fragments from which $Ni_2(C_2H_4)$ may be considered to be derived. Specifically, we will consider first the bonding and low-lying states of the Ni_2^{12} and $Ni(C_2H_4)^{13}$ molecules, noting the features common to both of them that make the formation of $Ni_2(C_2H_4)$ a logical next step in the sequence of nickel-ethylene cluster complexes.

A. $Ni(C_2H_4)$. The zerovalent $Ni(C_2H_4)$ complex provides a simple framework for probing the nature of the metal-olefin bond. This complex has been studied recently using several theoretical approaches including extended Hückel (EH)^{5b} and $X\alpha$ -SW.^{6b} The description given below is based on GVB and CI calculations, the basic details of which have been reported elsewhere.¹³

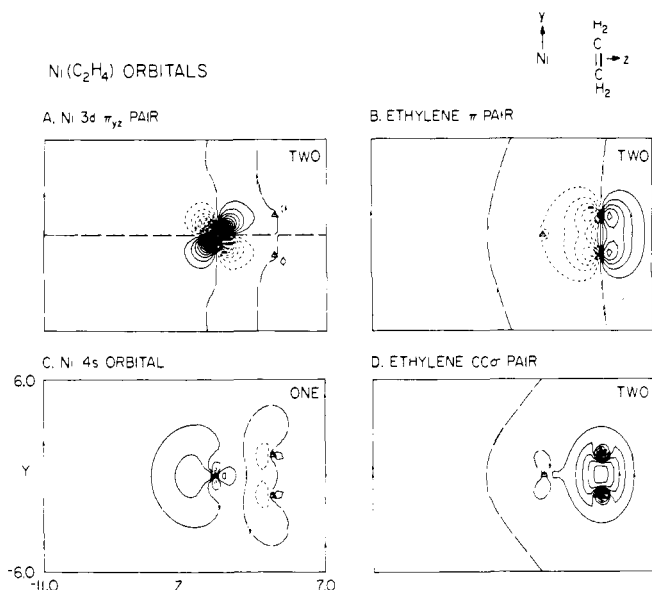


Figure 11. Bonding orbitals for the $Ni(C_2H_4)$ complex from GVB calculations. The plotting plane does not contain the H atoms. Long dashes indicate nodal lines.

We will first consider what happens when the separate ethylene molecule and Ni atom are brought together. The ethylene π orbital interacts first with the diffuse 4s orbital of the Ni atom. The ground state (3F) of the Ni atom²⁸ has a doubly occupied 4s orbital that leads to repulsive interactions with the ethylene π orbital, making strong bonding unfavorable. The first excited state of the Ni atom (3D) has a singly occupied 4s orbital and is only 0.03 eV above the 3F state. This singly occupied orbital can more readily mix in 4p character, hybridizing away from the Ni-ethylene bonding region and thus minimizing repulsive interactions with the π orbital. The ethylene molecule is able to move close enough to the Ni atom to allow the π orbital to delocalize slightly, resulting in a net bonding interaction. This situation is depicted in Figure 11 where bonding orbitals for the system are shown.

The interaction of the $3d^9$ shell of 3D Ni with the ethylene is more subtle. These orbitals are very contracted in comparison with the 4s orbital, and the ethylene is unable to move close enough to the Ni atom to interact strongly with it. The singly occupied orbital in the ground state configuration is a $d\delta$ orbital due to the intraatomic coupling effect^{12,31,35} which allows optimum hybridization of the 4s orbital. This orbital and the remaining doubly occupied orbitals are all localized on the Ni atom. The interactions of these 3d orbitals with the ethylene ligand are so weak in fact that the five states of $Ni(C_2H_4)$ formed by placing the single 3d electron in each of the five d orbitals span a range of only 0.5 eV above the 3A_1 ground state. In particular, there is almost no delocalization of the $3d\pi_{yz}$ orbital into the ethylene π^* orbital, a feature that is in direct contradiction with the standard Dewar-Chart-Duncanson¹⁵ model for metal-olefin bonds (see Figure 11).

This description leads to a particularly simple model for the Ni-olefin bond. With the hybridization of the 4s orbital away from the ethylene molecule, a $3d^9$ shell (largely unperturbed from atomic Ni) is left partially exposed. The ethylene π orbital is drawn toward this slightly electropositive center, its final distance (and binding energy) being limited by its interaction with the 4s orbital.

With this type of model, little perturbation of the ethylene molecule would be expected. The CC bond distance (see Figure 12) is found to increase by only 0.02 Å to 1.36 Å and the CH bonds bend back only 2° out of the ethylene molecular plane. Experimentally, this appears as a reduction in the ν_{CC} from

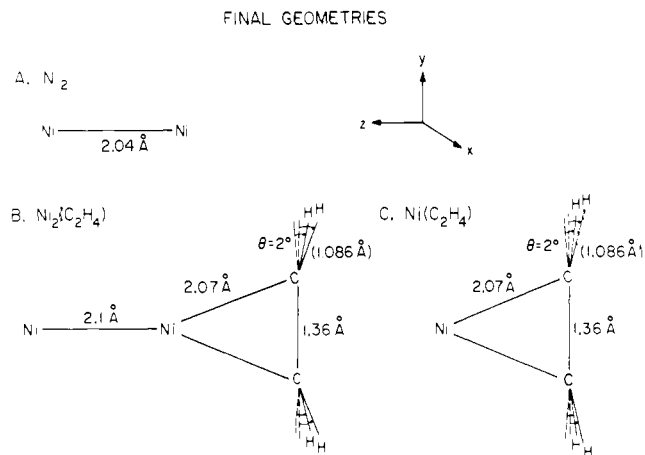


Figure 12. Final geometries for the complexes discussed here from GVB-CI calculations. No change was found in CC distance for $Ni_2(C_2H_4)$ relative to $Ni(C_2H_4)$, so no further optimization of HCC angles was attempted.

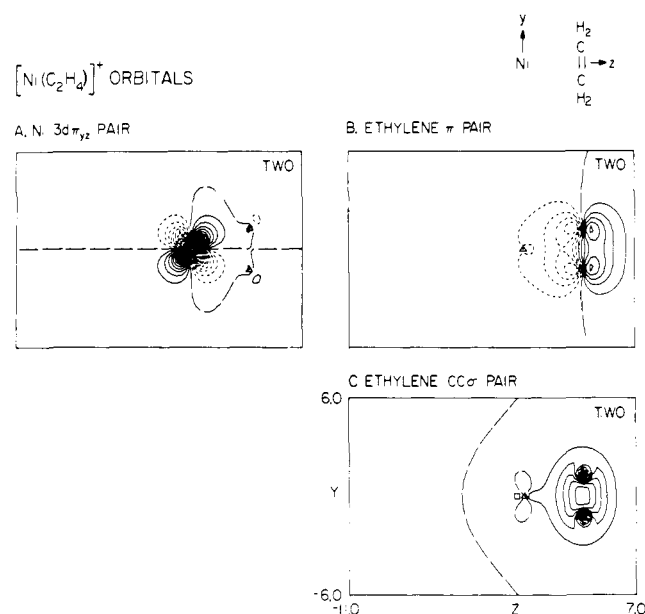


Figure 13. Bonding orbitals for the $[Ni(C_2H_4)]^+$ complex showing the effect of removing the 4s orbital. Note the slight increase in delocalization of the π orbital toward Ni atom.

1612 cm^{-1} for pure ethylene in Ar to the observed value of 1496 cm^{-1} for $Ni(C_2H_4)$ and a corresponding reduction of δ_{CH_2} from 1243 to 1158 cm^{-1} . These findings are also consistent with the photoemission data^{3d} for chemisorbed ethylene mentioned above.

It should be noted here that the strength of the bonding interaction is strongly dependent upon the presence of the 4s orbital. For the zerovalent complex of the optimum geometry, a binding energy of only 14.2 kcal is obtained. Removal of the 4s electron to form an Ni(I) complex leads to significant changes. The repulsive $4s-\pi(C_2H_4)$ interaction is eliminated, leading to an increase in the binding energy, at the same geometry, to almost 60 kcal. An examination of bonding orbitals for the $[Ni(C_2H_4)]^+$ complex, shown in Figure 13, indicates that only minor shape changes result, with a slightly greater π orbital delocalization toward the Ni atom. Removal of the 4s electron increases the electropositive character of the Ni atom as experienced by the olefin π bond, producing the increased binding energy.

B. Ni_2 . A similar approach may be used to describe the bonding in the nickel dimer and a complete discussion will

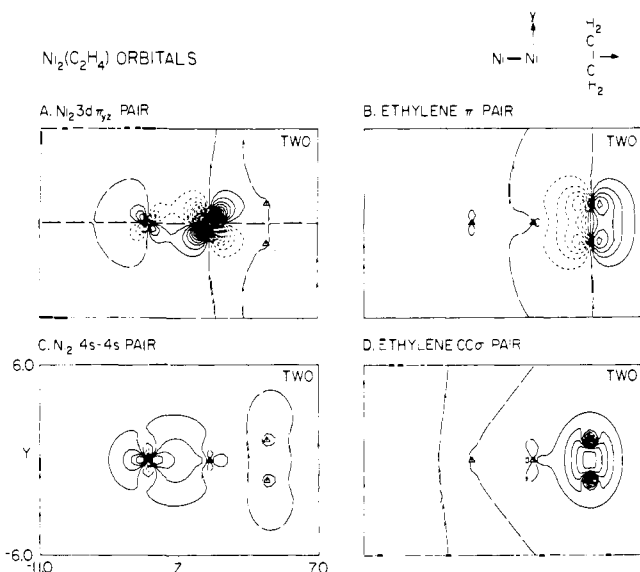


Figure 14. Bonding orbitals for the $\text{Ni}_2(\pi\text{-C}_2\text{H}_4)$ complex. The scale is the same as that used in Figure 11. Long dashes indicate nodal lines.

appear elsewhere.¹² Briefly, since the combination of two Ni atoms in their ^3F ground state configurations would lead to repulsive interactions between the doubly occupied 4s orbitals, the lowest states of Ni_2 are formed by combining the Ni atoms in their $4s^1 3d^9$ (^3D) states. As a result, there are 50 low-lying states (25 singlets and 25 triplets) that arise from considering the different spin couplings and possible occupations of the singly occupied 3d orbital on each center. The lowest of these involve singly occupied δ orbitals on each center, leading to extremely low overlap between δ orbitals on opposite centers. As a result, the lowest triplet state ($^3\Sigma_g^-$) and the lowest singlet state ($^1\Gamma_g$) are essentially degenerate. At the optimum bond distance for Ni_2 , the 3d orbitals interact very weakly, and the system is well described as a 4s-4s single-bonded molecule.

C. $\text{Ni}_2(\text{C}_2\text{H}_4)$. The essential point to be gained from the above discussion, as it relates to $\text{Ni}_2(\text{C}_2\text{H}_4)$, is that the Ni atoms of both Ni_2 and $\text{Ni}(\text{C}_2\text{H}_4)$ have the same electronic configuration. In $\text{Ni}(\text{C}_2\text{H}_4)$ the singly occupied 4s orbital is hybridized away from the C_2H_4 region and is triplet coupled to a singly occupied 3d δ orbital. As described above, this is precisely the configuration most favorable for formation of an Ni-Ni bond. Thus it is expected that the most stable conformation for the $\text{Ni}_2(\text{C}_2\text{H}_4)$ system would involve an ethylene unit π coordinated "end on" to the Ni_2 dimer. In Figure 12 are shown the optimum geometries for the $\text{Ni}_2^3\Sigma_g^-$, $\text{Ni}(\text{C}_2\text{H}_4)^3\text{A}_1$, and $\text{Ni}_2(\text{C}_2\text{H}_4)^3\text{A}_2$ systems obtained from generalized valence bond calculations. In the case of $\text{Ni}_2(\text{C}_2\text{H}_4)$, both the Ni-Ni and CC bond distances were optimized. There was essentially no change (less than 0.01 Å) in the CC distance relative to $\text{Ni}(\text{C}_2\text{H}_4)$. The Ni-Ni distance increased by 0.1 Å relative to Ni_2 to a value of 2.10 Å. The reasons for this may be seen by examining Figure 14 where orbitals for the $\text{Ni}_2(\text{C}_2\text{H}_4)$ system are shown. The 4s-4s bond of the Ni unit is polarized away from the ethylene molecule, just as for $\text{Ni}(\text{C}_2\text{H}_4)$. This polarization allows a slightly larger exposure of the 3d⁹ shell of the central Ni atom to the C_2H_4 as evidenced by the increase in binding energy for $\text{Ni}_2(\text{C}_2\text{H}_4)$ to 27.2 kcal. It is this distortion of the 4s-4s bonding orbital that leads to the increase in Ni-Ni distance.

As implied by Figure 14, there is little change in the nature of the Ni-olefin bond upon coordination of the second Ni atom. This is consistent with the results of the matrix infrared ex-

periments described in section II. The slight increase in exposure of the 3d⁹ shell of the Ni atom upon adding the second Ni atom produces opposing effects on ν_{CC} and δ_{CH_2} . The delocalization of the π orbital toward the Ni atom increases slightly, weakening the CC bond as is reflected in the decrease of ν_{CC} from 1499 to 1488 cm^{-1} . Similarly, the slightly bent CH bonds may relax toward the free molecule equilibrium owing to the reduction in repulsive interactions with the 4s orbital. The value of δ_{CH_2} then should move toward the free matrix ethylene value of 1243 cm^{-1} ; an increase from 1160 to 1208 cm^{-1} is noted experimentally.

At this point, it is worthwhile to draw on the bonding description presented above and to attempt tentative assignment of the intense UV transitions noted earlier for $\text{Ni}(\text{C}_2\text{H}_4)$ and $\text{Ni}_2(\text{C}_2\text{H}_4)$. To aid in characterizing these bands, it is helpful to draw on further experimental information. In Table II we show the position of the dominant band for a variety of mononuclear complexes of alkyl-substituted olefins, listed by decreasing transition energy. Included in this table are the gas-phase frequencies for the $^1(\pi \rightarrow \pi^*)$ transition of each olefin.³² In almost all cases, the trend toward decreasing energy for the Ni-olefin bands is paralleled by decreasing $^1(\pi \rightarrow \pi^*)$ transition frequencies. A correlation is suggested between the position of the virtual π^* level of the free olefins and the corresponding transition energy of the complex. There are several transitions that could lead to such a correlation: (1) ligand $\pi \rightarrow \pi^*$, (2) $\text{M}4s \rightarrow \text{ligand } \pi^*$, (3) $\text{M}3d \rightarrow \text{ligand } \pi^*$, (4) $\text{M}4s \rightarrow 4p_y$, and (5) $\text{M}3d \rightarrow 4p_y$. The distinction between (2) and (4) [or (3) and (5)] is small; certainly a transition that may be classified as $3d \rightarrow 4p_y$ will possess some degree of delocalization of the $4p_y$ into the ethylene π^* (and hence its inclusion in the list above). In fact, certain of these may be eliminated as possibilities. A simple ligand, $\pi \rightarrow \pi^*$, occurring at 7.6 eV³³ for free ethylene, will be shifted to far lower energies in the $\text{Ni}(\text{C}_2\text{H}_4)$ complex. This transition leaves a singly occupied π orbital which may bond to the singly occupied Ni 4s orbital. The strength of such a bond may be estimated from consideration of $[\text{Ni}(\text{C}_2\text{H}_4)]^+$ where the ethylene is bound by ~60 kcal. Preliminary calculations place this ($\pi\pi^*$) state at less than 2 eV above the $^3\text{A}_1$ ground state for $\text{Ni}(\text{C}_2\text{H}_4)$. In addition, it should be noted that the final state description for this ($\pi\pi^*$) state will be essentially identical with that expected of (2) [and thus (4)]. In each case, an occupation of $(\pi)^2(\pi^*)^1(3d)^9(4s)^0$ is expected for the upper state [where it is assumed that a $(4s-\pi)$ bond is indistinguishable from a $(\pi)^2 4s^0$ occupation]. Thus the arguments leading to rejection of (1) apply to (2) and (4) as well. Only (3) and (5) above do not perturb the $(4s)^1(\pi)^2$ configuration of the ground state and will be expected at energies similar to the atomic Ni($3d \rightarrow 4p$) transitions.²⁸ Preliminary calculations place the $3d \rightarrow 4p_y$ transition for $\text{Ni}(\text{C}_2\text{H}_4)$ at 6.1 eV, reasonably close to the observed value of 3.8 eV. Delocalization into the ethylene π^* is extensive, allowing classification of this state as formally $3d \rightarrow \pi^*$ MLCT (metal-ligand charge transfer). Since $\text{Ni}(\text{C}_2\text{H}_4)$ has a triplet ground state, to maintain spin symmetry in this transition it is necessary to pair the π^* and Ni 4s orbitals into a net singlet (the 3d⁸ shell is left in a ^3F state), an unfavorable coupling. Such is not the case for $\text{Cu}(\text{C}_2\text{H}_4)$, which has a $^2\text{A}_1$ ground state. As a result, the $^2\text{B}_2$ excited state of $\text{Cu}(\text{C}_2\text{H}_4)$ requires no open-shell singlet coupling of orbitals and is stabilized relative to the analogous atomic $^2(3d \rightarrow 4p_y)$ state; consequently, the corresponding transition appears at 3.2 eV.⁵¹ Similarly for $[\text{Cu}(\text{C}_2\text{H}_4)]^+$, the excited state is strongly bonding, reducing the atomic $^2(3d \rightarrow 4p_y)$ transition²⁸ by 2 eV to 5.6 eV.⁵¹ For $\text{Ni}_2(\text{C}_2\text{H}_4)$, there should be transitions similar to those observed for $\text{Ni}_2(3d \rightarrow 4p_\pi)$, producing a partial $\text{Ni}_2 \pi$ bond in addition to the higher energy MLCT transition. Thus we tentatively assign the intense 243-nm band as a MLCT transition, which here is blue shifted relative to $\text{Ni}(\text{C}_2\text{H}_4)$ as a re-

Table II. Ultraviolet-Visible Spectroscopic Data for a Selection of Ni(olefin) Complexes in Argon Matrices²³

olefin	Ni-olefin band position, cm^{-1}	rel energy, cm^{-1}	gas phase olefin ${}^1(\pi \rightarrow \pi^*)$ frequency, cm^{-1}	rel energy cm^{-1}
C_2H_4	31 250	0	6700	0
C_3H_6	30 910	-340	58 000	-3700
<i>cis</i> -but-2-ene	30 770	-480	57 470	-4230
<i>trans</i> -but-2-ene	30 675	-575	57 140	-4560
1-butene	30 630	-620	57 800	-3900
isobutene	30 440	-810	54 350	-7350

Table III. Ultraviolet-Visible Spectroscopic Data for $Ni(C_2H_4)$ and $Ni_2(C_2H_4)$ in Argon Matrices

$C_2H_4/Ar \approx 1/50$ $C_2H_4/Ar \approx 1/50^a$, $Ni/Ar \approx 1/10^4$, $Ni/Ar \approx 2/10^3$,		
nm	nm	assignment
320 ^b (s)	320 ^b (w)	MLCT: $Ni(C_2H_4)$
280 (w)	280 (mwsh)	MLCT: $Ni(C_2H_4)_2$
	243 (s)	MLCT: $Ni_2(C_2H_4)$
230 (mw)		MLCT: $Ni(C_2H_4)_3$

^a Depositions at higher Ni/Ar ratios and higher temperatures (20–25 K) show the growth of a band at roughly 370 nm concomitant with a general broadening of the spectra. This band and possible overlap in the region of 240 nm are tentatively ascribed to $Ni_2(C_2H_4)_2$ (see text). ^b The band initially ascribed to $Ni(C_2H_4)$ at 280 nm^{8e} was subsequently found to be the MLCT of $Ni(C_2H_4)_2$. The 320-nm band had been obscured by the absorptions of unreacted Ni atoms. This will be more fully detailed in a forthcoming report on Ni/olefin cocondensations.^{8g}

sult of the greater stabilization of the 3d levels in $Ni_2(C_2H_4)$. The band positions for both species, along with their tentative assignments, are collected for comparison in Table III.

D. Computational Details. All calculations on $Ni(C_2H_4)$ and $Ni_2(C_2H_4)$ employed the effective potential of Melius et al.³⁴ as modified by Sollenberger et al.³⁵ to replace the argon core of the Ni atom. This allowed truncation of the Ni basis set to include only the four most diffuse s functions from Wachters³⁶ Ni basis set, contracted "double ζ ". The 3d basis consisted of Wachters' five d functions contracted using atomic coefficients for the ${}^3D(4d^13d^9)$ state to a single basis function of each type. A single 4p Gaussian ($\alpha = 0.1$) was added to the Ni basis to allow hybridization of the 4s orbital. The ethylene basis set was the 9s/5p basis of Huzinaga³⁷ contracted to 3s/2p by Dunning³⁸ and augmented with a single set of d polarization functions ($\alpha = 0.6769$) on each C. All calculations on $Ni(C_2H_4)$ utilized the GVB(1)-PP wave function³⁹ where correlation effects were included in the ethylene π bond. For $Ni_2(C_2H_4)$, a GVB(2)-PP description was used with correlation effects included for both the ethylene π bond and Ni_2 σ bond. The orbitals obtained from these calculations were used as a basis for CI calculations in which all excitations were allowed between orbitals describing GVB pairs along with single and double excitations of the remaining Ni and Ni_2 orbitals (this is denoted as GVB-CI). A summary of energies from GVB and GVB-CI calculations for the complexes discussed here is listed in Table IV.

IV. Discussion

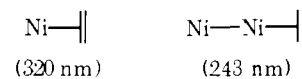
Probably the most significant results to emerge from the infrared and UV-matrix experiments concern (1) the minimal perturbation of the coordinated ethylene vibrational spectrum on placing the second nickel atom on $Ni(C_2H_4)$ to form $Ni_2(C_2H_4)$ and (2) the observation of a UV transition for $Ni(C_2H_4)$ at 320 nm which blue shifts to 243 nm on passing to $Ni_2(C_2H_4)$. In essence, one is observing the perturbation of

Table IV

complex	state	GVB ^a	GVB-CI ^a
$Ni_2(R = 2.1 \text{ \AA})$	${}^3\Sigma_g^-$	-81.0704 ^b	-81.0704
$Ni(C_2H_4)$	3A_2	-118.5820	-118.5822
$Ni_2(C_2H_4)$	3A_2	-159.1800	-159.1805
Ni	3D	-40.4943	-40.4943
C_2H_4	1A_1	-78.0668	-78.0668

^a All energies are in hartrees. ^b All calculations where Ni atoms are present employ an effective potential³⁵ replacing the Ar core of each Ni atom. The energies given reflect the absence of core contributions to total energies.

the electronic structure of π -bonded C_2H_4 on a single nickel atom site by a neighboring Ni atom as shown below:



By analogy with the electronic transitions for dinickel itself which occur in a similar energy range, the observation of an absorption at roughly 370 nm for $Ni_2(C_2H_4)_2$ can be considered to support the idea of a nickel-nickel bond in this binuclear complex. Presumably a corresponding band for $Ni_2(C_2H_4)$ is either too weak to be observed or is hidden by other spectral features. Furthermore, the relatively small frequency perturbation of the ν_{CC} and δ_{CH_2} (aside from drastic band broadening effects) on passing into the $Ni_n(C_2H_4)$ regime with $n \geq 2$ and the noticeable resemblance of these infrared spectra to those of chemisorbed C_2H_4 lend experimental credence to the proposal that cluster species like $Ni_2(C_2H_4)$ are valuable models for evaluating the properties of surface complexes, at least for the case of alkenes. However, our experiments do not allow us to dismiss the possibility that π - $Ni_2(C_2H_4)$ is the kinetically stable form under the conditions of our matrix experiments (10–45 K) and that higher temperature matrix experiments could lead to conversion to a di- σ - $Ni_2(C_2H_4)$ complex. Therefore, we cannot eliminate the possible existence of di- σ - $Ni_2(C_2H_4)$, and, as previously noted,⁷ the di- σ -surface complex may well play the role of a reaction intermediate for various surface reactions owing to its weaker C-C bond. In this context we recall that Soma^{10d} recently observed only the π -surface complex for C_2H_4 chemisorbed on Al_2O_3 supported Pd and Pt catalysts at -86 °C. However, when the catalyst was allowed to gradually warm up, infrared bands, which he assigned to the di- σ bonded surface species, were observed to grow in at 2940/2880 and 1338 cm^{-1} . Similarly, Broden and Rhodin⁴⁰ have recently noted that the photoemission spectrum of ethylene chemisorbed on Ir(100) (1×5) exhibits warmup behavior consistent with a transition from a simple π -bonded form to a stretched or even fragmented carbon-carbon bond species. For the finite complex being considered here, it is possible to consider directly the competing energetics of π vs di- σ bonded forms. Under the conditions of our experiment, it is necessary to consider the formation of $Ni_2(C_2H_4)$ as resulting from the interaction of ethylene with

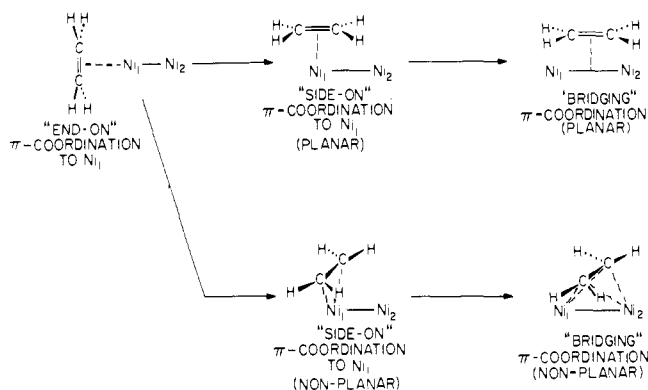
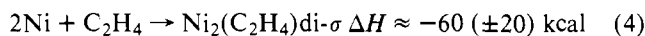
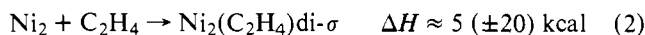


Figure 15. Other possible geometries for $\text{Ni}_2(\text{C}_2\text{H}_4)$ as they might be reached through ligand migration. Note that the initial movement of the ligand is different for the two indicated pathways.

either Ni atoms or Ni_2 . From similar calculations (GVB-CI) on the analogous di- σ $\text{Ni}_2(\text{C}_2\text{H}_2)$ species,⁴¹ the strength of the NiC σ bond may be estimated at 60 (± 10) kcal for the olefinic system. With this information, the following comparisons may be made:



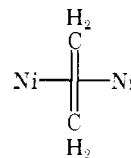
Within the estimates of error given, the di- σ and π forms appear competitive. Formation of the di- σ form requires breakage of the π bond, and, unlike the π complex, formation of this species will involve a significant (< 20 kcal) activation energy. For the finite complex, then, the di- σ form should be thermally inaccessible.

Within the context of this discussion, it is worthwhile to consider the importance of other possible geometries for the $\text{Ni}_2(\text{C}_2\text{H}_4)$ complex. Along with the di- σ form, the μ -bridging configuration, with the carbon-carbon bond oriented perpendicular to the Ni-Ni bond, is often suggested for chemisorbed species.⁴² This form, well known for finite-cluster metal-alkyne complexes,⁴³ is less favorable for the analogous olefinic systems. The reasons for this may be seen by examining the nature of the bonding involved. When in the μ -bridging configuration, acetylenic species may form two π -coordination bonds of the type described in this study, one to each metal atom.⁴³ The 4s orbitals on each Ni atom polarize away from the acetylene, reducing the Ni_2 bonding overlap. There is no corresponding scheme for ethylene in this orientation. This may be understood by considering the energy surface for the transformation from the π form to both the μ -bridging and planar forms shown in Figure 15. The initial step, moving the ethylene in its π -coordinate form around to either of the two "side-on" configurations (with respect to the Ni_2 bond), should be endothermic. It is still possible to expose the electropositive 3d⁹ shell on the bonding Ni atom; however, to do so requires polarization of the 4s orbital associated with this atom in a direction away from the Ni_2 bond. Continuing to move the ethylene to either final position (see Figure 15) requires polarization of both 4s bonding orbitals away from the ethylene and their region of maximum overlap. Unlike acetylene, there is no compensation for this disruptive polarization to be had through formation of a second (~ 15 kcal) π bond.⁴⁴ Thus, we would expect this "ligand migration" to be endothermic with respect to the "end-on" π configuration. It is important to re-

iterate at this point that these arguments for both di- σ and μ forms are specific to the finite cluster complex. The presence of neighboring Ni atoms at the metal surface is sufficient to obscure both the importance of 4s overlap between neighboring atoms and the related thermochemical arguments.

In addition to the coordination scheme presented here, there is also a "metallocyclopropyl" form⁴⁵ in which the Ni assumes a $^3\text{F}(s^2d^8)$ configuration and forms a σ bond to each C. (This state is quite distinct from that of an ethylene π bond to an s^1d^9 Ni.) Forming individual Ni-C σ bonds between 4s electrons on the Ni and "sp²" hybrid orbitals on the ethylene produces a ring compound more analogous to cyclopropane. Aside from the rather different spectral properties to be expected from such a form,⁴⁶ it is energetically unfavorable to couple the Ni 4s electrons in this manner. (Attempts to calculate the orbitals for this form collapsed to the Ni-C₂H₄ π complex.) The Ni 4s orbitals are very diffuse (see Figure 11) and when coupled into separate σ bonds favor a linear configuration to minimize overlap between bond pairs. Thus, a "ring strain" is expected to be an even greater problem for the metallocycle than its cycloalkane analogue.

Finally, we may consider the coordination of a second Ni atom to $\text{Ni}(\text{C}_2\text{H}_4)$ across the ethylene CC bond to form a second weak π bond and a planar $\text{Ni}(\text{C}_2\text{H}_4)\text{Ni}$ "di- π " complex:



Such a system should exhibit spectral properties very similar to those of $\text{Ni}(\text{C}_2\text{H}_4)$ as little additional perturbation of the ethylene would be expected relative to $\text{Ni}(\text{C}_2\text{H}_4)$. However, coordination of the second Ni in this position is exothermic by only ~ 15 kcal, while formation of the Ni_2 bond yields 65 kcal. Unless steric and/or kinetic effects in the matrix are particularly important, this structure should not be favored.

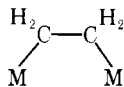
The $\text{Ni}(\text{C}_2\text{H}_4)$ and $\text{Ni}_2(\text{C}_2\text{H}_4)$ systems have been examined by other methods, notably $X\alpha$ -SW^{6b,7} and EH.^{5b} Both of these methods use approximate Hamiltonians in their description of the molecules and at best should reproduce the Hartree-Fock (HF) description. The EH result favors the di- σ form by over 25 kcal, yielding a binding energy of 68 kcal per bond.

The study presented here finds a direct parallel in the $X\alpha$ -SW work. In two separate studies, the $\text{Ni}(\text{C}_2\text{H}_4)$ ^{6b} and $\text{Ni}_2(\text{C}_2\text{H}_4)$ ⁷ complexes were considered, both in the π -coordinate orientation. In each case, a bonding description very similar to the Dewar-Chatt-Duncanson¹⁵ model emerges, with significant interaction of the Ni 3d π_{yz} and ethylene π^* orbitals, although the authors appear to disagree on the assignment of these two orbitals. This interaction is balanced by donation from the ethylene π orbital into a Ni σ orbital. This result is similar to that obtained from HF calculations, and the strong interactions between 3d and ethylene π orbitals may be attributed to the overestimation of ionic character inherent in the HF description. The di- σ form is also considered in this study, and although no energetic comparisons may be made, the π -coordinate geometry was favored by its better correspondence with known ethylene chemisorption data.

V. Relevance of the Spectroscopic Data for $\text{Ni}(\text{C}_2\text{H}_4)_n$ and $\text{Ni}_2(\text{C}_2\text{H}_4)_m$ to the Problem of Ethylene Chemisorbed on Supported and Unsupported Metal Catalysts

Most mechanisms proposed for the heterogeneous catalytic hydrogenation of ethylene have required specific assumptions concerning the nature of chemisorbed ethylene and of its participation in hydrogenation. The literature on this subject

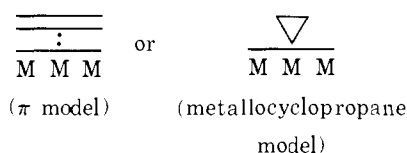
is voluminous and, because of a number of recent conflicting reports, often confusing. In brief, several spectroscopic^{10a,b} and chemical studies^{17,47} conclude that the species giving rise to the strong infrared ν_{CH_2} band of ethylene chemisorbed onto Ni, Pd, Pt, and Rh is a σ -bonded, associatively adsorbed species of the type



(where M denotes a surface metal atom). From these early reports one learns that this type of surface complex is probably the precursor of gaseous ethane as evidenced by its reaction with hydrogen. However, these conclusions appear somewhat unclear in the light of two recent infrared spectroscopic reports^{10c,d} of a π -bonded ethylene molecule on Pd and Pt surfaces. Controlled addition of hydrogen showed that the bands of the π surface complex disappeared most rapidly followed by bands from the σ -bonded species.^{10c} Although we are not surprised by the identification and enhanced reactivity of the π surface complex toward hydrogen, we are concerned about the validity of a di- σ assignment for the other surface ethylene complex.

The history of the di- σ vibrational assignment appears to originate with the work of Sheppard et al.^{10a} The basis of his model rests heavily on a correlation which is supposed to exist between the sp^n state of hybridization of the carbon atom attached to surface metal atom sites and the respective ν_{CH} stretching frequencies. This correlation has as its premise the trend in the ν_{CH} frequencies of C_2H_2 (3330 cm^{-1}), C_2H_4 (3050 cm^{-1}), and C_2H_6 (2940 cm^{-1}) and the red shifting of these ν_{CH} modes on complexation. Thus for C_2H_4 chemisorbed on silica-supported Ni at $-78^\circ C$, the presence of a strong ν_{CH_2} absorption at 2870 cm^{-1} has been taken to be diagnostic for the di- σ surface complexed form of ethylene. One worrisome aspect of this type of IR-spectroscopic-structural correlation relates to the nonobservation of carbon-carbon stretching modes which would have been characteristic of the di- σ type of surface complex. Rather more disquieting, however, are the results of our work with localized bonding models for chemisorbed ethylene, which show ν_{CH_2} stretching modes for $M(\pi-C_2H_4)_{1,2,3}$ in the range 2960–2800 cm^{-1} (for $M = Ni^{8e}$ or Pd^{48}) and at 2908/2880 cm^{-1} for the more pertinent model complexes $Ni_2(\pi-C_2H_4)_{1,2}$. However, there exists no compelling evidence for us to ascribe these binary metal-ethylene complexes to anything other than π complexes.

One must keep in mind that the vibrational data for localized bonding models such as $M(C_2H_4)_n$ and $M_2(C_2H_4)_m$ can only be used as a guide to understanding the electronic and geometric structures of the π -chemisorbed form of ethylene on metal surfaces. Moreover, the clear distinction between π coordination and metallocyclopropane bonding found for



$Ni(C_2H_4)$ may not persist for the metal surface owing to the effect of interactions with the other metal atoms of the surface. Indeed, the type of bonding could depend upon surface site and may be radically modified for sites at steps (edges) or kinks (corners) rather than on plateaus.⁴⁹ This is an intriguing possibility and one that we hope will be entertained in future work involving surface alkenes.

Acknowledgments. We (G.A.O. and W.J.P.) gratefully acknowledge the financial assistance of the National Research Council of Canada (NRCC), (W.A.G. and T.H.U.) the Na-

tional Science Foundation (Grant DMR74-04965), (G.A.O. and W.J.P.) the Atkinson Foundation, the Connaught Foundation, Imperial Oil of Canada, Erindale College, and the Lash Miller Chemistry Laboratories. W.J.P. expresses his appreciation to the NRCC for a graduate scholarship.

References and Notes

- (1) Sherman Fairchild Distinguished Scholar, 1977, California Institute of Technology.
- (2) Contribution No. 5623.
- (3) (a) T. E. Madey, J. T. Yates, Jr., D. R. Sandstrom, and R. J. H. Voorhoeve in "Solid State Chemistry", Vol. 2, N. B. Hannay, Ed., 1976, p 1; (b) L. H. Little, "Infrared Spectra of Adsorbed Species", Academic Press, New York, N.Y., 1966; (c) M. L. Hair, "Infrared Spectroscopy in Surface Chemistry", Marcel Dekker, New York, N.Y., 1967; (d) J. E. Demuth and D. E. Eastman, *Phys. Rev. Lett.*, **32**, 1123 (1974); (e) H. Conrad, G. Ertl, H. Knözinger, J. Küppers, and E. E. Latta, *Chem. Phys. Lett.*, **42**, 115 (1976); (f) G. C. Bond, "Catalysis by Metals", Academic Press, New York, N.Y., 1962, and references cited therein.
- (4) (a) R. Ugo, *Catal. Rev.*, **11**, 225 (1975); (b) E. L. Muetterties, *Bull. Soc. Chim. Belg.*, **84**, 959 (1975); **85**, 7 (1976); *Science*, **196**, 839 (1977); (c) G. A. Ozin, *Acc. Chem. Res.*, **10**, 21 (1977), and references cited therein.
- (5) (a) A. Anderson and R. Hoffmann, *J. Chem. Phys.*, **61**, 4545 (1974); (b) A. Anderson, *J. Am. Chem. Soc.*, **99**, 696 (1977); *J. Chem. Phys.*, **65**, 1729 (1976); **64**, 4046 (1976); *Chem. Phys. Lett.*, **35**, 498 (1975); (c) R. C. Baetzold, *J. Chem. Phys.*, **55**, 4363 (1971); *J. Catal.*, **29**, 129 (1973); *Surf. Sci.*, **51**, 1 (1975); (d) R. C. Baetzold and R. E. Mack, *J. Chem. Phys.*, **62**, 1513 (1975); (e) G. Blyholder, *Surf. Sci.*, **42**, 249 (1974), and references cited therein.
- (6) (a) R. P. Messmer, S. K. Knudson, K. H. Johnson, J. B. Diamond, and C. Y. Yang, *Phys. Rev. Sect. B*, **13**, 1396 (1976); (b) R. P. Messmer in "The Physical Basis for Heterogeneous Catalysis", E. Dragulis and R. I. Jaffee, Ed., Plenum Press, New York, N.Y., 1975; (c) K. H. Johnson and R. P. Messmer, *Int. J. Quantum Chem. Symp.*, **10**, 147 (1976); (d) N. Rösch and K. H. Johnson, *J. Mol. Catal.*, **1**, 395 (1976); (e) C. F. Melius, J. W. Moskowitz, A. P. Mortola, M. B. Baillie, and M. A. Ratner, *Surf. Sci.*, **59**, 279 (1976); (f) I. P. Batra and O. Robaux, *J. Vac. Sci. Technol.*, **12**, 242 (1975), and references cited therein.
- (7) N. Rösch and T. N. Rhodin, *Faraday Discuss. Chem. Soc.*, **58**, 28 (1975).
- (8) (a) G. A. Ozin and M. Moskovits in "Cryochemistry", G. A. Ozin and M. Moskovits, Ed., Wiley, New York, N.Y., 1976; (b) G. A. Ozin and W. J. Power, *Inorg. Chem.*, **16**, 212 (1977); (c) D. McIntosh and G. A. Ozin, *ibid.*, **16**, 51 (1977); (d) D. McIntosh and G. A. Ozin, *ibid.*, **16**, 59 (1977); (e) H. Huber, W. J. Power, and G. A. Ozin, *J. Am. Chem. Soc.*, **98**, 6508 (1976); (f) J. E. Hulse and M. Moskovits, *Surf. Sci.*, **57**, 125 (1976), and references cited therein; (g) W. J. Power and G. A. Ozin, manuscript in preparation.
- (9) See, for example, M. O. Thomas, W. R. Pretzer, B. F. Beler, F. J. Hirsekorn, and E. L. Muetterties, *J. Am. Chem. Soc.*, **99**, 743 (1977), and references cited therein.
- (10) (a) B. A. Morrow and N. Sheppard, *J. Phys. Chem.*, **70**, 2406 (1966); *Proc. R. Soc. London, Ser. A*, **311**, 391 (1969); (b) J. Erkelens and T. Liefkens, *J. Catal.*, **8**, 36 (1967); (c) J. D. Prentice, A. Lesiunas, and N. Sheppard, *J. Chem. Soc., Chem. Commun.*, **76** (1976); (d) Y. Soma, *ibid.*, 1004 (1976); (e) G. Blyholder, D. Shihabi, W. V. Wyatt, and R. Bartlett, *J. Catal.*, **43**, 122 (1976); (f) H. A. Pearce and N. Sheppard, *Surf. Sci.*, **59**, 205 (1976); (g) G. Casalone, M. G. Cattania, M. Simonetta, and M. Tesccari, *ibid.*, **62**, 321 (1977), and references cited therein.
- (11) J. E. Hulse and M. Moskovits, *J. Chem. Phys.*, **66**, 3988 (1977).
- (12) T. H. Upton and W. A. Goddard III, *J. Am. Chem. Soc.*, in press.
- (13) T. H. Upton and W. A. Goddard III, *J. Am. Chem. Soc.*, **100**, 321 (1978).
- (14) J. E. Demuth and D. E. Eastman, *Phys. Rev. Sect. B*, **13**, 1523 (1976).
- (15) J. Chatt and L. A. Duncanson, *J. Chem. Soc.*, 2939 (1953); M. J. S. Dewar, *Bull. Soc. Chim. Fr.*, **18**, C71 (1971).
- (16) G. I. Jenkins and E. K. Rideal, *J. Chem. Soc.*, 2941 (1955).
- (17) J. H. Sinfelt, *Adv. Catal.*, **23**, 91 (1973).
- (18) W. Koltzbücher and G. A. Ozin, *Inorg. Chem.*, **15**, 292 (1976).
- (19) E. P. Kündig, M. Moskovits, and G. A. Ozin, *J. Mol. Struct.*, **14**, 137 (1972).
- (20) M. Moskovitz and G. A. Ozin, *Appl. Spectrosc.*, **26**, 487 (1972).
- (21) K. Fischer, K. Jonas, and G. Wilke, *Angew. Chem.*, **85**, 629 (1973); *Angew. Chem., Int. Ed. Engl.*, **12**, 565 (1973).
- (22) (a) See E. P. Kündig and G. A. Ozin in ref 8a, first communicated at the Merck Symposium on Metal Atoms in Chemical Synthesis, Darmstadt, Germany, May 1974; (b) P. L. Timms, communicated in a paper given at the C.I.C. Meeting on Chemistry under Extreme Conditions, Toronto, Canada, June 1975; (c) R. M. Atkins, R. McKenzie, P. L. Timms, and T. W. Turney, *J. Chem. Soc., Chem. Commun.*, 764 (1975).
- (23) G. A. Ozin and W. J. Power, manuscript in preparation.
- (24) E. P. Kündig, M. Moskovits, and G. A. Ozin, *Angew. Chem., Int. Ed. Engl.*, **14**, 292 (1975).
- (25) See D. M. Gruen in ref 8a.
- (26) (a) R. Busby, W. Koltzbücher, and G. A. Ozin, *J. Am. Chem. Soc.*, **98**, 4013 (1976); (b) A. Ford, H. Huber, W. Koltzbücher, E. P. Kündig, M. Moskovits, and G. A. Ozin, *J. Chem. Phys.*, **66**, 524 (1977); (c) E. P. Kündig, M. Moskovits, and G. A. Ozin, *Nature (London)*, **254**, 503 (1975); (d) G. A. Ozin, *Appl. Spectrosc.*, **30**, 573 (1976).
- (27) A. Kant, *J. Chem. Phys.*, **41**, 3806 (1964).
- (28) C. E. Moore, "Atomic Energy Levels", *Natl. Bur. Stand. (U.S.), Circ.*, **No. 467** (1949).

